Statistics of Multipath Component Clustering in an Office Environment

E. Tanghe*, W. Joseph*†, M. Lienard†, A. Nasr†, P. Stefanut†, L. Martens*, and P. Degauque†
*Ghent University / IBBT, Dept. of Information Technology
Gaston Crommenlaan 8 box 201, B-9050 Ghent, Belgium, e-mail: emmeric.tanghe@intec.ugent.be
†University of Lille, IEMN, Group TELICE
Bldg. P3, F 59655 Villeneuve d'Ascq, France, e-mail: martine.lienard@univ-lille1.fr

***Abstract*—In this paper, directional MIMO measurements in an indoor office environment are presented. A 5-D ESPRIT estimation algorithm is used to extract parameters associated with discrete propagation paths, such as their azimuth of arrival, azimuth of departure, delay, and power. The estimated path parameters are grouped into clusters using the statistical K-power-means algorithm. Statistical distributions are determined for the path parameters within individual clusters and for their change between clusters. To validate the distributional choices, the goodness-of-fit to the proposed distributions is verified using statistical hypothesis tests with sufficient power.**

I. Introduction

The last decade, the demand for high throughput wireless communication has increased enormously. To meet the ever increasing requirements for reliable communication with high throughput, novel wireless technologies have to be considered. A promising approach to increase wireless capacity is to exploit the spatial structure of wireless channels through multiple-input multiple-output (MIMO) techniques. High throughput MIMO specifications are already being included in wireless standards, most notably IEEE 802.11n, IEEE 802.16e, and 3GPP Long Term Evolution (LTE).

The potential benefits of implementing MIMO are highly dependent on the sort of propagation environment. Therefore, the development of propagation channel models is indispensable. In this paper, the geometry-based stochastic type of MIMO channel model is considered. This kind of model presents a statistical distribution for the propagation path parameters (e.g., their direction of arrival, direction of departure, delay, etc.). Geometry-based stochastic channel models use propagation path clusters in their description: paths with similar propagation parameters are grouped into clusters. An example of this type of channel model is the COST 273 model [1].

This work investigates the statistics of path powers, azimuths of arrival (AoA), azimuths of departure (AoD), and delays in an indoor office environment. For this, MIMO channel sounding measurements with a virtual antenna array are carried out on a typical office floor. Parameters of propagation paths are extracted from measurement data and are subsequently grouped into clusters using an automatic clustering algorithm. In this paper, statistical distributions are provided for the clustered propagation path parameters.

II. Measurements

The measurement setup for the MIMO measurements is shown in Fig. 1. A network analyzer is used to measure the complex channel frequency response for a set of transmitting and receiving antenna positions. The channel is probed at 1601 evenly spaced frequency points in a range from 3 GHz to 3.5 GHz. As transmitting (Tx) and receiving antenna (Rx), broadband omnidirectional biconical antennas with a nominal gain of 1 dBi are used. To be able to perform measurements for large Tx-Rx separations, one port of the network analyzer is connected to the Tx through an RF/optical link with an optical fiber of length 500 m. The RF signal sent into the Tx and the RF signal coming from the Rx are both amplified using an amplifier with an average gain of 37 dB.

Measurements are performed using a virtual MIMO array. The virtual array is created by moving the antennas to predefined positions along rails in two directions in the horizontal plane using stepper motors. Both Tx and Rx are moved along 10 by 4 virtual uniform rectangular arrays (URAs), and are polarized vertically and positioned at a height of 1.80 m during measurements. The URA elements are spaced 4.29 cm apart, which is equal to half a wavelength at 3.5 GHz in order to avoid spatial aliasing. The stepper motor controllers, as well as the network analyzer, are controlled by a personal computer (PC). At each of the 1600 ($10 \times 4 \times 10 \times 4$) combinations of Tx and Rx positioning along the URAs, the network analyser measures the S_{21} scattering parameter ten times (i.e., 10 time

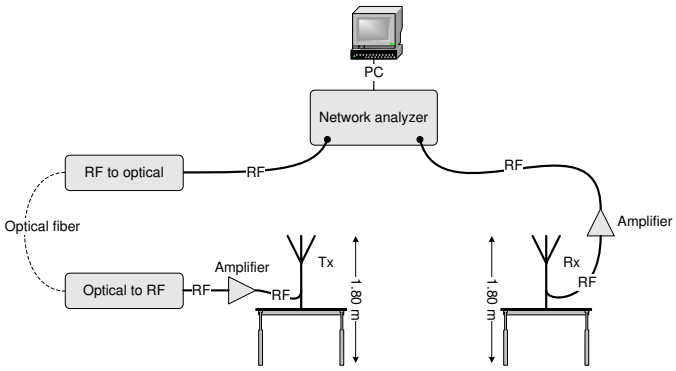

Fig. 1. Measurement setup

observations).

The measurements are carried out on the first floor of an office building. Fig. 2 presents a floor plan of the measurement environment, along with some relevant dimensions. Most inner walls are plasterboard. Fig. 2 also shows locations of the Tx and Rx during measurements. A total of 9 MIMO measurements are performed, their Tx and Rx locations indicated by couples of Tx_i and Rx_i ($i = 1, \ldots, 9$). Measurements are executed in both line-of-sight (LoS) and non line-of-sight (nLoS) conditions: measurement locations 1, 5, and 6 are LoS.

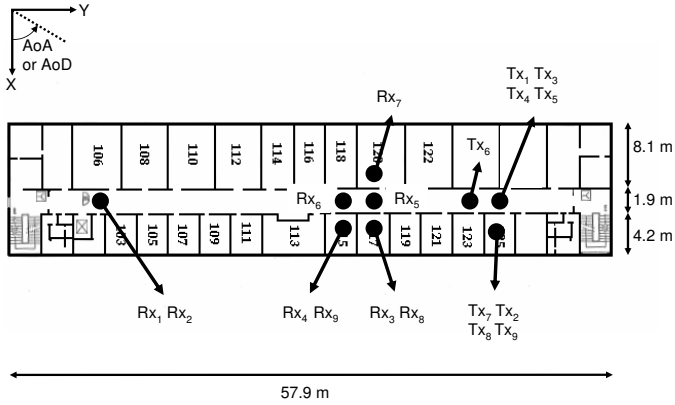

Fig. 2. Floor plan of the measurement environment with Tx and Rx locations

III. Data processing

A. Extraction of specular paths

The power, azimuth of arrival (AoA), azimuth of departure (AoD), and delay parameters of propagation paths or multipath components (MPCs) are extracted from measurement data using the 5-D unitary ESPRIT (Estimation of Signal Parameters via Rotational Invariance Techniques) algorithm [2]. The coordinate system with respect to which AoA and AoD are defined is shown in Fig. 2.

URAs allow easy application of the spatial smoothing technique to increase the number of observations [3]. We choose sub-URAs with dimensions $2/3$ of the length in each direction of the original 10 by 4 URA, i.e., 7 by 3 sub-URAs. In total at both link ends, 64 different 7 by 3 sub-URAs can be found, thereby increasing the number of observations by a factor of 64. Together with the previously mentioned 10 time observations, the total number of available observations per measurement location is 640. From the measured frequency points, 10 equally spaced frequencies are selected from 3.5 GHz down for use with the ESPRIT algorithm. The considered constant spacing between these frequencies is 4 MHz. With this choice, the maximum resolvable path length is 75 m, which is expected to be large enough to limit possible aliasing in the delay domain. Summarizing, 5-D unitary ESPRIT is applied to 640 observations of a 5-D vector space of size $7 \times 3 \times 7 \times 3 \times 10$.

The ESPRIT algorithm is used to estimate the 100 most strongest paths from measurement data. The estimated MPCs are postprocessed in the delay domain by considering the power delay profile (PDP). For a typical PDP, power is concentrated at small delays while at large delays only the noise floor remains. In our measurements, the noise floor is set to the power of the MPC with the largest delay. Following, all MPCs with power less than the noise floor plus a noise threshold of 6 dB are omitted from further analysis. Fig. 3(a) shows a scatter plot of detected MPCs versus their AoA, AoD, and delay for measurement location 7 (nLoS). The power on a dB-scale of each MPC is indicated by a color.

B. Clustering of specular paths

For our data, automatic joint clustering of AoA, AoD, and delay is performed using the K-power-means algorithm [4]. The K-power-means algorithm result is in agreement with the COST 273 definition of a cluster as a set of MPCs with similar propagation characteristics [1]. Because some parameters for clustering are circular, multipath component distance (MCD) is used as the distance measure for clustering [4].

For each measurement location, the number of clusters for the K-power-means algorithm is varied between 2 and 10. The optimal number of clusters is selected using the Kim-Parks index [5]. The number of clusters according to Kim-Parks index varies from 3 to 8 between measurement locations, and for all MIMO measurements combined, a total of 45 clusters are found (16 clusters from LoS and 29 clusters from nLoS measurements). Next, to ease the statistical analysis, clearly outlying MPCs are removed from each cluster using the shapeprune algorithm detailed in [4]. Fig. 3(b) shows clustering results for measurement location 7 (nLoS). MPCs grouped into different clusters are shown with different marker shapes and colors (in total 4 clusters).

IV. Signal model

For the analysis of the within-cluster and between-cluster propagation path parameters, the following basic signal model is used. For one of the measurement locations, the complex received envelope $\boldsymbol{h}\left(\phi^A, \phi^D, \tau\right)$ is written as function of the propagation path parameters: ϕ^A denotes the AoA, ϕ^D the AoD, and τ is the path delay. The use of MPC clusters is reflected in the complex envelope's notation:

$$\boldsymbol{h}\left(\phi^A, \phi^D, \tau\right) = \sum_{c=1}^{n_C} \sum_{k=1}^{n_{P,c}} \boldsymbol{A_{c,k}} \cdot \delta\left(\phi^A - \Phi_{c,k}^A\right) \cdot \delta\left(\phi^D - \Phi_{c,k}^D\right) \cdot \delta\left(\tau - T_{c,k}\right) \quad (1)$$

In (1), n_C is the number of clusters and $n_{P,c}$ is the number of MPCs within cluster c. For the k-th propagation path in cluster c, $\boldsymbol{A_{c,k}}$ is its received complex amplitude, $\Phi_{c,k}^A$ and $\Phi_{c,k}^D$ are its AoA and AoD, and $T_{c,k}$ is its delay. $\delta\left(.\right)$ denotes the Dirac delta function. We also define $P_{c,k}$ as the power of path k in cluster c, i.e., $P_{c,k} = E\left[\left|\boldsymbol{A_{c,k}}\right|^2\right]$ where the expectation operator $E\left[\cdot\right]$ is taken over all 640 observations of $\boldsymbol{A_{c,k}}$. To allow statistical analysis of propagation parameters of all measurement locations collectively, the dependence of power $P_{c,k}$ and delay $T_{c,k}$ on distance is removed. Power is

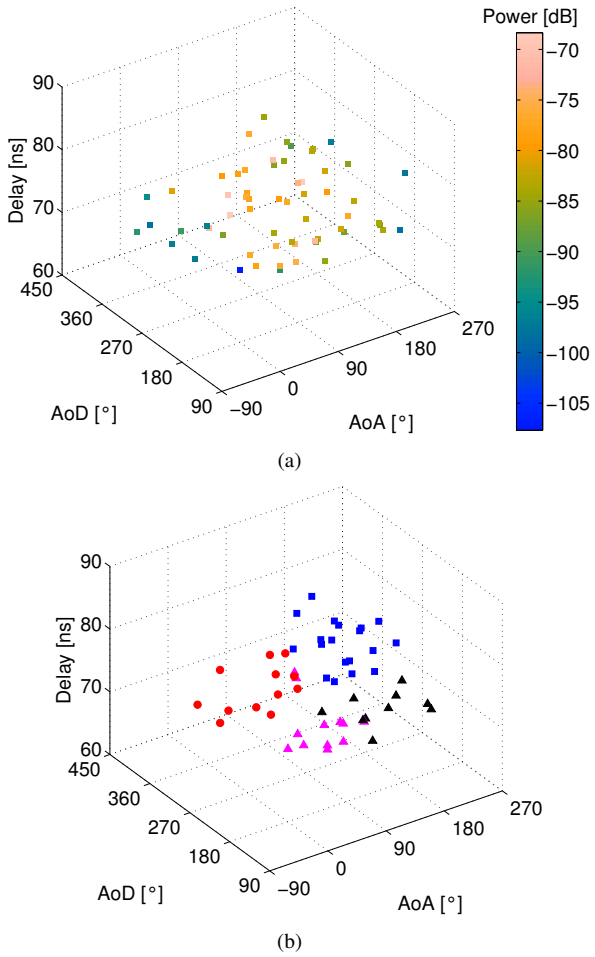

Fig. 3. MPC scatter plot (a) and clustering (b) for measurement location 7

rescaled such that the total received MPC power equals one and the origin of the delay axis is set to coincide with the first arriving MPC. Assuming larger values of c or k mean later arriving paths:

$$\sum_{c=1}^{n_C} \sum_{k=1}^{n_{P,c}} P_{c,k} = 1 \quad \text{and} \quad T_{1,1} = 0 \text{ ns} \tag{2}$$

Each of the propagation path parameters $P_{c,k}$, $\Phi^A_{c,k}$, $\Phi^D_{c,k}$, and $T_{c,k}$ are split up into a between-cluster and a within-cluster part as follows:

$$\begin{aligned} P_{c,k} &= p_c \, p_{c,k} & \Phi^A_{c,k} &= \phi^A_c + \phi^A_{c,k} \\ \Phi^D_{c,k} &= \phi^D_c + \phi^D_{c,k} & T_{c,k} &= \tau_c + \tau_{c,k} \end{aligned} \tag{3}$$

In (3), the parameters p_c, ϕ^A_c, ϕ^D_c, and τ_c denote *between-cluster* propagation parameters, and are representative for the *location* of each cluster in the power/AoA/AoD/delay parameter space. Also in (3), $p_{c,k}$, $\phi^A_{c,k}$, $\phi^D_{c,k}$, and $\tau_{c,k}$ are *within-cluster* propagation parameters. The within-cluster parameters can be seen as the deviations of individual paths from the cluster's location as dictated by the between-cluster parameters. The within-cluster parameters are therefore fully determined by the *spread* of power, AoA, AoD, and delay in each of the clusters. The following sections will work towards a statistical description of the between-cluster and within-cluster propagation parameters.

V. Statistical Distributions per Cluster

This section discusses the statistical distributions of $P_{c,k}$, $\Phi^A_{c,k}$, $\Phi^D_{c,k}$, and $T_{c,k}$ within each cluster. The proposed distributions are location-scale distributions: they are parameterized by a *location parameter*, which determines the distribution's location or shift, and a *scale parameter*, which determines the distribution's dispersion or spread.

A. Power $P_{c,k}$

A natural model for the fading of MPC powers $P_{c,k}$ in cluster c is the lognormal fading model. For cluster c, it is investigated if the samples $P_{c,k}$ on a dB-scale could originate from a normal distribution. This normal distribution is parameterized by the mean μ_c (*location parameter*) and the standard deviation σ_c (*scale parameter*) of $P_{c,k}$ in dB.

Composite normality of $P_{c,k}$ [dB] is assessed with a few statistical tests in literature such as the Anderson-Darling (AD) test, the Shapiro-Wilk (SW) test, and the Henze-Zirkler (HZ) test. Multiple tests for normality are executed as no uniformly most powerful test exists against all possible alternative distributions. Of the 45 clusters in this measurement campaign, normality of $P_{c,k}$ [dB] is retained at the 5% significance level for 39, 38, and 40 clusters with the AD, SW, and HZ tests, respectively. For the 45 clusters, average p-values are 0.38 (AD), 0.43 (SW), and 0.44 (HZ). Concluding, normality for $P_{c,k}$ [dB] is assumed in the following, as the majority of clusters pass the different goodness-of-fit tests.

B. Azimuths of arrival $\Phi^A_{c,k}$ and departure $\Phi^D_{c,k}$

In literature, various distributions are proposed for the azimuth angles $\Phi^A_{c,k}$ and $\Phi^D_{c,k}$ within a certain cluster c, among which the normal distribution and the Laplacian distribution. Additionally, we consider the von Mises distribution. The von Mises distribution can be thought of as an analogue of the normal distribution for circular data. For the AoAs $\Phi^A_{c,k}$ in cluster c, the von Mises probability density function (pdf) $p_{\text{vM}}\left(\Phi^A_{c,k}\,;\,\alpha^A_c, \kappa^A_c\right)$ is given as:

$$p_{\text{vM}}\left(\Phi^A_{c,k}\,;\,\alpha^A_c, \kappa^A_c\right) = \frac{\exp\left(\kappa^A_c \cos\left(\Phi^A_{c,k} - \alpha^A_c\right)\right)}{2\pi I_0\left(\kappa^A_c\right)} \tag{4}$$

In (4), $I_0(\cdot)$ is the modified Bessel function of the zeroth order. The two parameters that characterize the von Mises pdf are α^A_c, the circular mean of $\Phi^A_{c,k}$ (*location parameter*), and κ^A_c, which is a measure of concentration of $\Phi^A_{c,k}$ angles around α^A_c (*scale parameter*). For the von Mises pdf of AoDs $\Phi^D_{c,k}$ in cluster c, an expression analogous to (4) can be written.

The most fit distribution is determined by performing simple likelihood ratio tests (LRTs): the statistical distribution which renders the largest likelihood is most appropriate for describing the azimuth angle statistics for that cluster. For the 45 clusters in this measurement campaign, all LRTs decided in favor

of the von Mises distribution for both $\Phi_{c,k}^A$ and $\Phi_{c,k}^D$. We therefore conclude that the von Mises distribution is most fit for describing the statistics of azimuth angles within clusters.

C. Delay $T_{c,k}$

Delays $T_{c,k}$ within cluster c are modeled according the principle laid out by the well-known, cluster-based Saleh-Valuenzuela (SV) model [6]. Herein, the waiting time between the arrival of two consecutive MPCs within a certain cluster is modeled by an exponential distribution. For the MPCs in cluster c (assuming the delays are ordered such that $T_{c,1} < T_{c,2} < \ldots < T_{c,n_{P,c}}$), the exponential pdf $p_{\exp}\left(T_{c,k} \mid T_{c,k-1}\,;\,\lambda_c\right)$ as function of the delay $T_{c,k}$ of the k-th MPC, given that the $(k-1)$-th MPC arrived at known delay $T_{c,k-1}$, is written as:

$$p_{\exp}\left(T_{c,k} \mid T_{c,k-1}\,;\,\lambda_c\right) = \frac{1}{\lambda_c}\exp\left(-\frac{T_{c,k}-T_{c,k-1}}{\lambda_c}\right) \quad (5)$$

In (5), the exponential distribution has the parameter λ_c which corresponds to the mean waiting time between consecutive MPCs in cluster c (*scale parameter*). An additional distributional parameter θ_c is defined as the delay of the first arriving path in cluster c, i.e., $\theta_c = T_{c,1}$ (*location parameter*).

The plausibility of an exponential distribution for the arrival times $T_{c,k}$ is then validated by executing an Anderson-Darling (AD) goodness-of-fit test for composite exponentiality. For the 45 clusters in the measurement campaign, the minimum, average, and maximum p-values associated with the AD test are equal to 0.06, 0.40, and 0.92, respectively. This means that, at the 5% significance level, all 45 clusters retain exponentiality.

VI. Statistics of the distributional parameters

This section models the between-cluster and within-cluster propagation parameters as defined in (3). The propagation parameters are fully determined by the distributional parameters of the location-scale distributions of Section V. In the following, the *between-cluster propagation parameters* are identified with the *location parameters* of these distributions, i.e., for cluster c:

$$\phi_c^A \triangleq \alpha_c^A \quad \phi_c^D \triangleq \alpha_c^D \quad \tau_c \triangleq \theta_c \quad p_c \triangleq \mu_c \quad (6)$$

The *within-cluster propagation parameters* are characterized by the *scale parameters* of the distributions, i.e., for the MPCs in cluster c:

$$\phi_{c,k}^A \rightarrow \kappa_c^A \quad \phi_{c,k}^D \rightarrow \kappa_c^D \quad \tau_{c,k} \rightarrow \lambda_c \quad p_{c,k} \rightarrow \sigma_c \quad (7)$$

In the following, the statistics of the distributional parameters are discussed. In this section, distinction is made between distributional parameters originating from LoS and nLoS measurements.

A. Location parameters (between-cluster)

1) Cluster angular means ϕ_c^A and ϕ_c^D: The suitability of a uniform distribution in $(-\pi, \pi]$ for modeling ϕ_c^A and ϕ_c^D is investigated. No distinction is made between LoS and nLoS, as the uniform distribution is not parameterized by any distributional parameter (which could change between these two circumstances). The premise of a uniform distribution is validated through a statistical hypothesis test, namely Rao's spacing test for uniformity. For both the 45 cluster mean AoAs ϕ_c^A and the 45 cluster mean AoDs ϕ_c^D, Rao's spacing test retained the null hypothesis of a uniform distribution at the 5% significance level (p-values of 0.67 and 0.14, respectively).

2) Cluster onset τ_c: We adopt the Saleh-Valenzuela model for the between-cluster delay: the waiting time between the onsets $\tau_c - \tau_{c-1}$ of two consecutively arriving clusters is modeled by an exponential distribution [6]. This exponential distribution is fully parameterized by the mean of waiting times $\tau_c - \tau_{c-1}$.

Under the assumption of an exponential distribution, it is first investigated if the mean waiting time between clusters differs between LoS and nLoS measurements. This done by executing the two-sample Anderson-Darling (AD) test, which assesses if $\tau_c - \tau_{c-1}$ grouped according to LoS or nLoS could both originate from the same statistical distribution. This test results in a p-value of 0.04, which is borderline significant at the 5% level and prompts us to distinguish between LoS and nLoS. Next, for LoS and nLoS separately, composite exponentiality of $\tau_c - \tau_{c-1}$ is verified using the one-sample AD test. An exponential distribution is accepted for both LoS and nLoS at the 5% significance level (p-values of 0.13 and 0.12, respectively). The mean of waiting times $\tau_c - \tau_{c-1}$ is estimated at 2.30 ns for LoS and 1.21 ns for nLoS.

3) Cluster mean power p_c: Significant correlation is found between cluster mean power p_c and cluster onset τ_c: Spearman's rank correlation coefficient is equal to -0.80 for LoS and -0.58 for nLoS, both are significant at the strict 1% level with p-values of $1.8 \cdot 10^{-4}$ for LoS and $9.7 \cdot 10^{-4}$ for nLoS. The Saleh-Valenzuela model proposes a linear decrease of the average p_c of MPC powers in dB with the cluster onset τ_c in ns [6]:

$$p_c = a_0 + a_1 \cdot \tau_c + a_2 \cdot D_c + a_3 \cdot \tau_c \cdot D_c + \epsilon_c \quad (8)$$

In the linear model (8), p_c is made dependent on τ_c and the dummy variable D_c. The value of D_c is one for clusters stemming from LoS measurements and is zero for nLoS clusters. As such, D_c accounts for possible changes in the intercept and slope of (8) between LoS and nLoS situations. Furthermore, a_0 through a_3 are regression parameters, and the term ϵ_c denotes the model's error for cluster c and is generally assumed to be zero-mean normally distributed. The regression parameters in (8) are estimated using a backward elimination procedure: simple t-tests are carried out on a_0 through a_3 to determine which of these regression parameters can assumed to be zero at the 5% significance level. The backward elimination procedure resulted in the following estimated regression parameters:

$$a_0 = -20.14 \quad a_1 = -0.81 \quad a_2 = 0 \quad a_3 = 0 \quad (9)$$

The standard deviation of ϵ_c in (8) is estimated at 4.72 dB. The coefficient of determination of the fitted model is equal to 0.42. In (9), it is noted that the regression parameters a_2 and a_3 associated with the dummy variable D_c are assumed

to be zero by the backward elimination procedure. This means that the form of the exponential and power law models is not significantly different between LoS and nLoS measurements. Fig. 4 shows a scatter plot of p_c versus τ_c along with the fitted linear model.

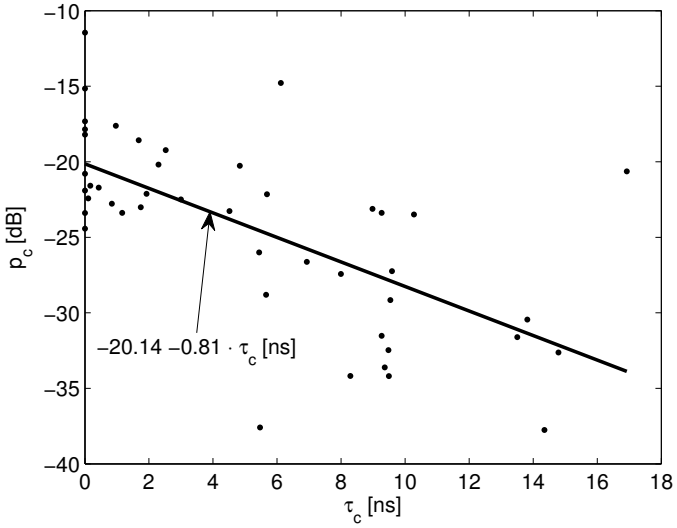

Fig. 4. Scatter plot of p_c versus τ_c and fitted linear model

B. Scale parameters (within-cluster)

To our knowledge, no examples of possible statistical distributions for the scale parameters exist in literature. We will therefore use the entropy-maximizing normal distribution to model these parameters. As the scale parameters can only take on positive values, they are first log-transformed to match the support of the normal distribution (i.e., any positive or non-positive number).

1) Cluster angular concentrations κ_c^A and κ_c^D: It is first investigated if the statistical distribution of κ_c^A (κ_c^D) differs significantly between LoS and nLoS measurements. For this, the two-sample Anderson-Darling (AD) test is used on obtained values of κ_c^A (κ_c^D) grouped according to LoS or nLoS. For both κ_c^A and κ_c^D, this test detects no difference between LoS and nLoS distributions at the 5% significance level (p-values of 0.16 and 0.20, respectively). Without making distinction between LoS and nLoS, the assumptions of normality for $\log\left(\kappa_c^A\right)$ and $\log\left(\kappa_c^D\right)$ are validated using the Anderson-Darling (AD), Shapiro-Wilk (SW), and Henze-Zirkler (HZ) tests. For $\log\left(\kappa_c^A\right)$, all three tests accepted normality at the 5% level with p-values of 0.37 (AD), 0.46 (SW), and 0.31 (HZ). The sample mean and sample standard deviation of $\log\left(\kappa_c^A\right)$ are equal to 0.50 and 0.33, respectively. Furthermore, normality is also accepted for $\log\left(\kappa_c^D\right)$ with p-values of 0.09 (AD), 0.14 (SW), and 0.59 (HZ). The sample mean and standard deviation of $\log\left(\kappa_c^D\right)$ equal 0.36 and 0.32, respectively.

2) Cluster mean waiting time between MPCs λ_c: It is first assessed whether λ_c (in ns) originating from LoS or nLoS measurements could have been drawn from the same statistical distribution. A two-sample AD test on λ_c grouped according to LoS or nLoS results in a p-value of 0.19, indicating no significant difference between LoS and nLoS at the 5% level. Next, normality for $\log(\lambda_c)$ without making distinction between LoS and nLoS is considered: AD, SW, and HZ hypothesis tests accepted normality at the 5% level with p-values of 0.13, 0.21, and 0.13, respectively. We therefore assume a normal distribution for $\log(\lambda_c)$: the sample mean and sample standard deviation of $\log(\lambda_c)$ are equal to 0.03 and 0.35, respectively.

3) Cluster standard deviation of power σ_c: For σ_c (in dB), a two-sample AD test decides there is no significant change in the statistical distribution of this parameter between LoS and nLoS measurements (p-value of 0.34). Normality for $\log(\sigma_c)$ is assessed with the AD, SW, and HZ hypothesis tests, all of which accepted normality at the 5% level (p-values of 0.61, 0.78, and 0.41, respectively). The sample mean and sample standard deviation of $\log(\sigma_c)$ are equal to 0.88 and 0.14, respectively.

VII. Conclusions

In this paper, the statistics of propagation path parameters including their azimuth of arrival, azimuth of departure, delay, and power, are determined in an indoor office environment. Path parameters are grouped into clusters. Statistical distributions and correlations are determined for the path parameters within individual clusters and for their change between clusters. As validation for the distributional choices, statistical goodness-of-fit tests are used.

Acknowledgment

W. Joseph is a Post-Doctoral Fellow of the FWO-V (Research Foundation - Flanders). This work was carried out within the frame of CISIT (International Campus on Safety and Intermodality in Transportation) and with the support of the FEDER funds, the French Ministry of research and the Region Nord Pas-de-Calais (France).

References

[1] L. M. Correia, *Mobile Broadband Multimedia Networks - Techniques, Models, and Tools for 4G*, 1st ed. Elsevier Ltd., 2006.

[2] M. Haardt, "Efficient One-, Two-, and Multidimensional High-Resolution Array Signal Processing," Ph.D. dissertation, Technische Universität München, Shaker Verlag GmbH, Aachen, DE, 1996.

[3] T. J. Shan, M. Wax, and T. Kailath, "On Spatial Smoothing for Direction-of-Arrival Estimation of Coherent Signals," *IEEE Transactions on Acoustics, Speech, and Signal Processing*, vol. 33, no. 4, pp. 806–811, August 1985.

[4] N. Czink, P. Cera, J. Salo, E. Bonek, J.-P. Nuutinen, and J. Ylitalo, "A Framework for Automatic Clustering of Parametric MIMO Channel Data Including Path Powers," in *IEEE Vehicular Technology Conference*, Montréal, CA, September 2006, pp. 1–5.

[5] D.-J. Kim, Y.-W. Park, and D.-J. Park, "A Novel Validity Index for Determination of the Optimal Number of Clusters," *IEICE Transactions on Information and Systems*, vol. E84-D, no. 2, pp. 281–285, February 2001.

[6] A. A. M. Saleh and R. A. Valenzuela, "A Statistical Model for Indoor Multipath Propagation," *IEEE Journal on Selected Areas in Communications*, vol. 5, no. 2, pp. 128–137, February 1987.